

Stephen F. Mueller^{a*}, Jonathan W. Mallard^a and Stephanie L. Shaw^b

^aTennessee Valley Authority, Muscle Shoals, Alabama

^bElectric Power Research Institute, Palo Alto, California

1. INTRODUCTION

Fugitive emissions are emitted gaseous or aerosol materials that do not pass through vents, stacks or other openings. These emissions can significantly affect air quality near a source and are regulated by federal and state agencies. By their nature, fugitive emissions are difficult to quantify. Various indirect techniques have been used to estimate emissions of particulate matter—from sources such as bare soils, aggregate storage piles or unpaved roads—and relate them to physical processes using empirical methods or mathematical modeling. Here we describe a study of fugitive particulate emissions from a coal pile.

This study often found enhanced particulate levels downwind of the pile in the absence of human activity even when measured wind speeds were below the threshold normally considered significant for wind erosion. Video evidence and measurements confirmed that dust clouds originated over the pile, particularly (but not exclusively) during the daytime when solar radiation levels were high.

Downwind measurements indicated natural particulate concentrations that were usually less than those observed when human disturbances affected the pile but were, nonetheless, important for separating natural from anthropogenic influences on dust generation. In the present context “dust” refers to particles smaller than 10 μm in size (PM_{10}).

2. PROCESSES AFFECTING NATURAL FUGITIVE EMISSIONS

2.1 Combustion

Coal piles are prone to spontaneous combustion and the risk of fires increases with the dust content. Western coals such as Powder River Basin (PRB) sub-bituminous coal are very dusty and especially prone to burning in storage (Nugroho et al., 2008). Coal

combustion in piles is usually a slow smoldering process (U.S. Environmental Protection Agency, 1978) and its smoke contains aerosols formed from gaseous combustion byproducts. Aerosols formed in this manner are typically $\ll 1 \mu\text{m}$ in diameter (Perera and Litton, 2009). Uptake of water vapor and other condensable gases will—along with particle coagulation—result in particle size growth but these particles generally remain in the so-called $\text{PM}_{2.5}$ size range (i.e., $< 2.5 \mu\text{m}$).

2.2 Wind

Wind erosion of particulate matter from soils and aggregate piles has been studied previously, either empirically (Cowherd et al., 1974; Saxton et al., 2000) or using modeling (Ono, 2006; Laurent et al., 2009; Harris and Davidson, 2009). Blended methods that used both modeling and observations have also been published (Gillette et al., 2004; Turpin and Harion, 2009). Dust emissions from aggregate storage piles are summarized in Cowherd et al. (1974), in Watson et al. (2000), and by the U.S. Environmental Protection Agency (EPA, 1995). A common issue examined across most of these studies is the extent to which wind speed affects emissions of PM_{10} size particles.

Cowherd et al. (1974) did not find a downwind concentration dependence on speed downwind of crushed rock and sand piles. They stated that, while measured concentrations were sensitive to the inverse of wind speed, emission rates likely had a positive dependence on speed and these two effects tended to obscure the true relationship. Saxton et al. (2000) and Gillette et al. (2004) assumed that PM_{10} emission flux from dry bare surfaces was proportional to the horizontal flux of windblown particles larger than 10 μm (i.e., by way of saltation or the “hopping” of large particles across the ground and the subsequent dislodging of smaller particles). For wind $> 5 \text{ m s}^{-1}$, Gillette et al. estimated PM_{10} wind erosion emission rates that ranged over 4 orders of magnitude during a 12-month study.

Laurent et al. (2009) summarized data from several erosion studies of exposed soils to show that the threshold wind friction velocity u_t^* (a predictor of particle entrainment from the

* Corresponding author address: Stephen F. Mueller, Tennessee Valley Authority, PO Box 1010, Muscle Shoals, AL 35662-1010; e-mail: sfmuller@tva.gov.

surface) has a minimum for particles 80 μm in size. Smaller particles resist erosion due to cohesive forces—electrostatic or those associated with the surface moisture—binding them with other surface particles. For 10 μm particles $u_t^* \approx 0.5 \text{ m s}^{-1}$ and exceeds 1 m s^{-1} for particles $\leq 2.5 \mu\text{m}$.

Harris and Davidson (2009) modeled physical processes resulting in the emission of 1-100 μm particles into the air by wind action. Particles $< 1 \mu\text{m}$ are expected to be bound too tightly to the surface to become airborne. Modeling indicated that aerodynamic forces were responsible for particle suspension when $u^* \leq 0.6 \text{ m s}^{-1}$. Above $u^* = 0.85 \text{ m s}^{-1}$ saltation was the cause of nearly all particle suspension. Harris and Davidson computed particulate emission rates that varied 4-5 orders of magnitude for different surface characteristics and $0.1 \leq u^* \leq 1.0 \text{ m s}^{-1}$. The simulated mass median diameter of emitted particles was 6-9 μm .

Turpin and Harion (2009) examined wind erosion from aggregate material piles using a computational fluid dynamics model of airflow over flat-topped piles of different configurations relative to the mean wind direction. The key parameter in analyzing this process is $\rho_u = u_s / u_r$ where u_s is wind speed at 0.25 m above the pile surface and u_r is a reference speed at 10 m. The value of ρ_u increases bottom to top along the windward edge of the pile and varies along lateral edges because of localized accelerations. Results also indicated the fraction of pile surface area subject to wind erosion due to variations in ρ_u . Pile heights varied 13-16 m and piles were about 75 m in length. With $u_r = 5 \text{ m s}^{-1}$ and wind gusts of up to 10 m s^{-1} , the fraction of total surface area of a pile theoretically subject to wind erosion varied between 46 and 55 percent across the different test configurations. These fractions decreased to 19-30 percent for the same mean wind but with wind gusts reduced by half.

Regulatory guidance on estimating wind-generated fugitive particulate emissions (EPA, 1995, and Watson et al., 2000) is consistent with the studies previously described. Specifically, wind emissions (a) are estimated to increase greatly with wind speed and gustiness (turbulence), (b) are sensitive to the dimensions and orientations of material stockpiles, and (c) tend to produce the greatest emission rates for particles near or just below 10 μm in size. Based on the EPA *AP-42 Emissions Handbook* (EPA, 1995 with subsequent updates), wind

erosion potential P_w from a dry aggregate storage pile is given by

$$P_w = 58(u^* - u_t^*)^2 + 25(u^* - u_t^*) \quad (1)$$

where u^* is the friction velocity on the storage pile and u_t^* is the threshold friction velocity for wind erosion ($P_w=0$ for $u^* \leq u_t^*$). The nonlinear relationship between P_w and u^* requires that the former be computed considering the spatial and temporal variation of u^* on the pile. *AP-42* provides guidance on how to estimate u^* variations due to pile geometry and orientation relative to wind direction. *AP-42* recommends using the peak wind speed measured at a short time interval to determine temporal variation in u^* . Given a peak wind speed at 10 m (u_{10}^+), it is possible to estimate a peak surface wind speed u_s^+ for air flowing over a pile as

$$u_s^+ = \rho_u u_{10}^+ \quad (2)$$

where ρ_u is the wind speed ratio described by Turpin and Harion (2009). For a typical storage pile, $\rho_u = 0.2$ near the pile base, rises to 0.9 just below the pile top and reaches 1.1 at the edge of the top where the wind accelerates as it crosses the pile. Assuming a pile roughness length of 0.5 cm and a log wind profile,

$$u^* = 0.10 u_s^+ \quad (3)$$

AP-42 lists u_t^* as ranging from 0.55 m s^{-1} (at the base of a crushed coal pile) to 1.12 m s^{-1} (uncrusted pile) giving a factor-of-2 difference in u_t^* on a coal pile. The former value is a lower limit in estimating wind erosion and is the threshold (along with the associated wind speed u_t) referenced later in this paper when sorting hours into “erosion” and “no erosion” categories.

2.3 Turbulence and Convection at Low Wind Speeds

While direct wind erosion of particles from soils and aggregate storage piles requires wind speeds with sufficient force to overcome binding forces, it is possible for dust to be lifted from a surface when mean wind speeds are lower than the established entrainment threshold. This occurs when a surface is subjected to the action of turbulent eddies. These eddies are likely to form on a sunny day over a dark-colored surface

such as a coal pile. An extreme example of turbulent eddies occurs in the form of dust devils. Even at night it is possible that dust may be entrained into the air above a storage pile by the action of air moving across the pile. This is somewhat counterintuitive given our expectation that nighttime winds and turbulence are lower than during the daytime.

Renno et al. (1998) describe dust devils as “heat engines” driven by sensible heat flux at the surface and formed from vorticity created by ambient wind shear. A dark coal pile is a strong absorber of solar radiation and the sloped pile surface warms fastest when the solar angle of incidence is optimally aligned to receive the maximum radiation exposure. Airflow over a pile can force localized wind shear depending on wind direction, pile shape and orientation. The

potential exists during daytime for a coal pile to experience conditions suitable for forming rotating convective turbulence and, in the extreme, dust devils. These microscale circulations potentially enhance localized wind speed near the surface and drive particle entrainment into the boundary layer.

3. FIELD MEASUREMENTS

A study of fugitive dust emissions from a coal storage pile was conducted June–November 2012 at the Gallatin electric power generating station operated by the Tennessee Valley Authority. The 6.6 ha coal pile has a long axis (NW–SE) of 380 m and a short axis (NE–SW) of 220 m. Pile topography is represented in Figure 1 using approximate 5-m height contours.

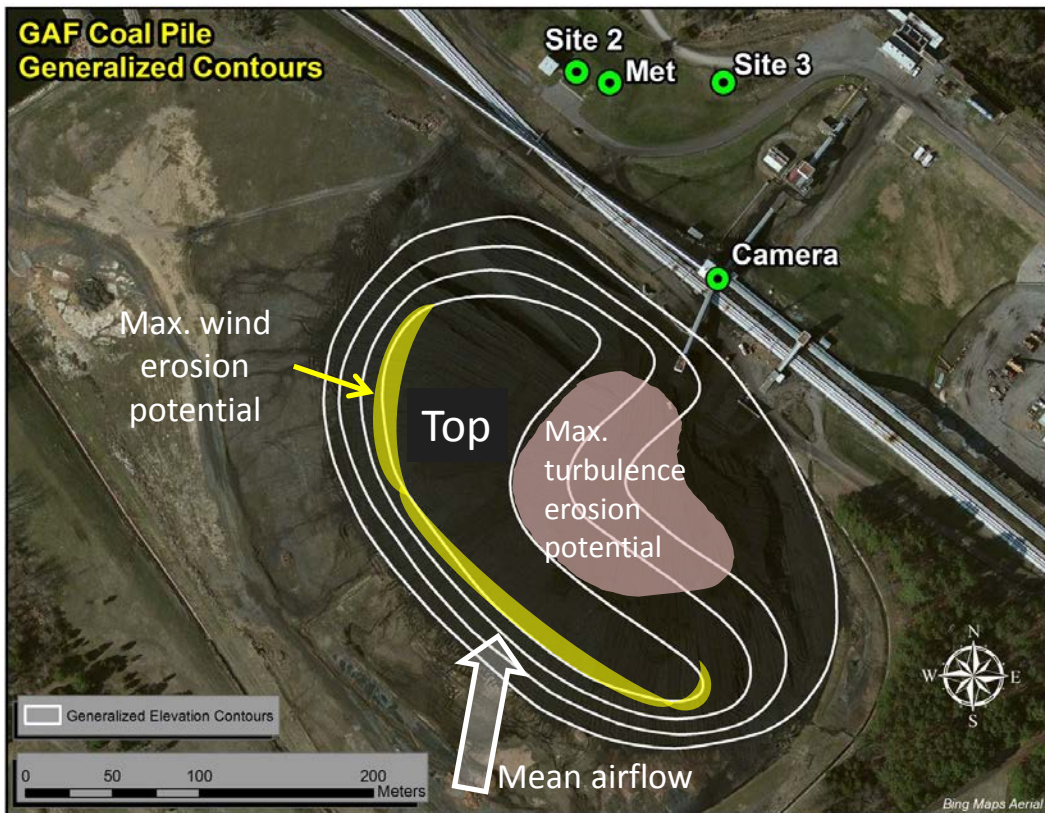


Figure 1. Approximate topographical representation of the coal pile. White lines denote approximate 5-m elevation contours but contour intervals are not necessarily to scale. The pile base elevation and pile boundary is marked by the outermost contour line. The innermost contour represents a relatively flat pile top but this was not always the case because of coal additions and subtractions. The yellow shaded area is the pile section most likely to experience particulate erosion from ambient wind. The area labeled “Max. turbulence erosion potential” is the area postulated to be the primary source of turbulence induced by localized solar heating and subsequent crosswinds (ambient and heating-generated). It is also the portion of the pile where dust devils were usually observed.

The actual height and contours change as coal is added to or removed. However, the pile is maintained roughly in a constant configuration as shown with a narrow flat top. During the latter part of the study (after 14 October 2012) there was a net removal of coal from the southern end of the pile but the maximum pile height (~15 m) changed only marginally.

Particulate measurements were made at one upwind (not seen in Figure 1) and two downwind sites (labeled “Site 2” and “Site 3” in Figure 1). A few infrequent minor sources of fugitive dust exist near the pile and their impacts on downwind measurements are considered insignificant. The northwest and southwest faces of the pile were steep such that bulldozers did not drive across them. Bulldozers did drive across the rest of the pile, including its top. The conditions examined here are for hours when air passed over the upwind face of the pile from southerly and westerly directions. According to AP-42, the highest wind accelerations under such conditions occur along the leading and lateral edges of the pile top, shown by the shaded region in Figure 1. These are the locations where direct wind removal of coal dust is most likely.

Meteorological data were collected at 1-min intervals while particulate concentrations represented 1-hour averages. Concentration differences of $<4 \mu\text{g m}^{-3}$ are not considered significant due to measurement limitations. Time lapse camera imagery was invaluable in detecting both human activity and natural phenomena occurring around the coal pile.

4. DATA ANALYSIS

Air blew across the coal pile and past sites 2 or 3 when the 10-m wind direction was between south-southeast and west-southwest (Table 1). Overall, these conditions occurred for about one quarter of the study. Wind speed varied only slightly by direction, averaging 2.4 m s^{-1} over all of these hours. Hours were eliminated from analysis when precipitation was measured at the site. The remaining hours were classified according to whether human activity was observed on or near the pile. Here we are concerned primarily with those hours when no activity occurred.

Over 800 rain-free hours occurred when airflow passed over the pile. Missing PM_{10} data slightly reduced the total number of hours analyzed. Table 2a summarizes differences between valid pairs of upwind and downwind

Table 1. Wind data summarized for hours when airflow potentially transported coal dust from the pile toward one or both downwind monitoring sites.

10-m Wind Direction	Frequency, %	Mean 10-m Speed, m s^{-1}	Maximum 10-m Speed, m s^{-1}
SSE	5.9	2.2	6.2
S	7.9	2.6	7.0
SSW	4.4	2.4	5.9
SW	3.5	2.1	5.1
WSW	4.2	2.4	5.8

PM_{10} concentrations. The fraction of all hours when the upwind PM_{10} measurement was significantly greater than the downwind measurement was 5.4 and 3.6 percent for sites 2 and 3, respectively. Upwind-downwind differences were negligible—i.e., within $\pm 4 \mu\text{g m}^{-3}$ —for 20 percent of all hours (both downwind sites). The downwind measurements were significantly greater than those upwind during three-quarters of all hours.

No human activity occurred near the pile for 35 and 37 percent of the observations at sites 3 and 2, respectively, across all PM_{10} observations with favorable wind directions for detecting coal pile impacts. In addition, positive contributions from the pile to downwind PM_{10} levels were measured during 50-58 percent of hours experiencing no human activity. The high frequency of positive contributions during non-activity hours was unexpected. We had assumed that the impact on excess downwind PM_{10} levels would be minor because wind speeds were generally below the erosion threshold. Also, coal fires were thought to be primarily sources of $\text{PM}_{2.5}$ and, thus, would not contribute substantially to PM_{10} mass. As shown in Table 2b, upwind-downwind $\text{PM}_{2.5}$ concentration differences were smaller compared to those for PM_{10} , implying a much smaller $\text{PM}_{2.5}$ coal pile signal. Hours without human activity produced no significant $\text{PM}_{2.5}$ differences about 60 percent of the time and showed a positive coal pile contribution only 23-28 percent of the time. Clearly, $\text{PM}_{2.5}$ levels associated with the pile are very small and represent a lower relative contribution for activity-free hours than found in the overall data set. Coal combustion likely makes a minor but unquantifiable contribution to naturally-occurring downwind PM_{10} mass.

Table 2. Total numbers of valid^a upwind-downwind pairs of concentration data in each of three categories for all hours and those without human activity on or near the coal pile.

(a) PM₁₀ data

Downwind Minus Upwind, δ	Site 2		Site 3	
	All hours	No activity	All hours	No activity
$<-4 \mu\text{g m}^{-3}$	42	37	29	8
$-4 \leq \delta < 4 \mu\text{g m}^{-3}$	151	105	160	111
$\geq 4 \mu\text{g m}^{-3}$	581	142	625	165
Total	774	284	814	284

(b) PM_{2.5} data

Downwind Minus Upwind, δ	Site 2		Site 3	
	All hours	No activity	All hours	No activity
$<-4 \mu\text{g m}^{-3}$	82	53	74	36
$-4 \leq \delta < 4 \mu\text{g m}^{-3}$	366	167	388	169
$\geq 4 \mu\text{g m}^{-3}$	256	64	278	79
Total	704	284	740	284

^aBoth concentration measurements were non-missing, hourly 10-m wind direction was between south-southeast and west-southwest, and no precipitation was measured.

One-minute meteorological data provided a detailed characterization of the boundary layer moving across the pile. Data include wind speed, direction, the standard deviation of the vertical wind component (σ_w), and the standard deviation of the horizontal wind direction (σ_θ). Other parameters were also measured or computed that had the potential to influence dust transport and downwind concentrations (see Table 3). Parameter $F(u)$ is the frequency with which the measured 1-min wind speed at level 2 (~10 m) exceeded the erosion threshold during an hour. This threshold, computed as the speed equivalent to the value of u_t^* previously described, was 5 m s^{-1} . For hours when u_t^* was exceeded, $F(u)$ averaged 0.14 with a maximum of 0.85. The nonlinear relationship between P_w and u^* (eq. 1) also suggests testing μ^2 [defined as $(u^* - u_t^*)^2$] as a potential predictor of downwind PM₁₀ levels.

The excess of particulate matter downwind (i.e., $C_{xs} = C_{dn} - C_{up}$, where C denotes the particulate concentration upwind, “up”, and downwind, “dn”) was assumed to be due to pile emissions. For hours when this difference was $\leq -4 \mu\text{g m}^{-3}$ we assumed that either a local source affected the upwind measurement or airflow variability was so large that a reliable excess concentration was indeterminate. In these cases C_{xs} was rendered unfit for coal pile emissions analysis. Measured variations in 1-min wind direction confirmed that airflow was seldom over the coal pile for all minutes of an

hour. Therefore, from the 1-min data we computed the fraction of time (f) during each hour that the airflow was over the pile. An adjusted C_{xs} (C_{xs}^*) was computed to remove the effect of airflow that did not cross the pile:

$$C_{xs}^* = C_{xs} / f \quad (4)$$

where f is the fraction of minutes during an hour with airflow crossing the pile. Average values of f for hours without human activity were 0.76 and 0.67 for sites 2 and 3, respectively. For cases when $f=0$, C_{xs}^* was not computable and the hour was dropped from the analysis. This adjustment provides for a more reliable comparison of different hours and produces a concentration value that is more easily analyzed for the dispersive influences on downwind concentrations. When C_{xs} was $0 \pm 4 \mu\text{g m}^{-3}$ we assumed that measurement sensitivity limited our ability to confidently quantify excess concentration levels. Thus, we treated near-zero values differently depending on whether $-4 < C_{xs} < 0$ or $0 < C_{xs} < 4 \mu\text{g m}^{-3}$ (i.e., arbitrarily setting all near-zero values to zero would introduce a bias—an excessive frequency of zero emissions—at the lower end of the C_{xs} distribution). The adjustment from (4) is meaningless for $C_{xs} < 0$ so in those cases $C_{xs}^* = 0$. However, C_{xs}^* was determined using (4) when $0 < C_{xs} < 4$ just as it was when $C_{xs} \geq 4$. Table 4 summarizes C_{xs} and C_{xs}^* for hours without coal pile activity. The maximum values listed for

Table 3. Parameters used to characterize conditions potentially affecting fugitive dust emissions from the coal pile and associated downwind particulate concentrations.^a

Parameter	Description	Level ^b
u	Horizontal mean wind speed	1 and 2
u^+	1-min maximum u	1 and 2
σ_u	Std. deviation of u	1 and 2
σ_u^+	1-min maximum σ_u	2
$F(u)$	Frequency that 1-min $u >$ wind erosion threshold during hour	2
μ^2	$(u^* - u_t^*)^2$	2
θ	Horizontal vector mean wind direction	1 and 2
θ_c	Angular deviation of θ from the direction of the pile center	1 and 2
σ_θ	Std. deviation of θ	1 and 2
σ_w	Std. deviation of vertical wind component	1 and 2
σ_w^+	1-min maximum σ_w	1 and 2
ε_{TK}	Turbulent kinetic energy	1 and 2
ε_{TK}^+	1-min maximum ε_{TK}	1 and 2
T	Air temperature	1 and 2
ξ	Relative humidity	1 and 2
ΔT	$T_2 - T_1$	
R_{sol}	Solar radiation flux	1
R_{net}	Net radiation flux (solar & infrared)	1
b_{scat}	Light scattering at 556 nm	2 m
σ_{bscat}	Std. deviation of light scattering	2 m
b_{scat}^+	1-min maximum b_{scat}	2 m
P	Precipitation amount over various time intervals	Surface
M_s	Soil moisture content ^c	-0.05 m
x_f	Fetch of airflow across the pile	
x	Distance from the pile edge to measured downwind concs.	

^aAll parameters are one hour averages unless stated otherwise.

^bLevel 1 is 2.3 m and level 2 is 9.6 m above the ground.

^cMeasured below the surface adjacent to the meteorological tower.

each site indicate a large range in excess concentrations compared to the mean, implying a long upper tail to the concentration distribution and results consistent with those previously reported for fly ash fugitive emissions (Mueller et al., 2013).

5. RESULTS

Video images revealed that small clouds of dust can occasionally be seen leaving the pile without human activity. Such observations are consistent with measurements when, in the absence of human activity, downwind PM₁₀ concentrations were significantly above

background. This suggests the possibility of natural dust emissions from the pile being associated with the action of turbulent flows occurring during periods of relatively light winds. In one instance a dust devil was seen by researchers to form and move across the pile lofting copious amounts of coal dust into the air. Photographic evidence of dust devils was also collected during the study. During one event the measured 10-m wind speed was $<2 \text{ m s}^{-1}$ and was from the north. The dust devil motion vector had an upwind component when compared with tower measurements. The occurrence of such extreme turbulent behavior implies airflow over the pile that does not always

Table 4. Average measured and adjusted excess concentrations ($\mu\text{g m}^{-3}$) at downwind monitors during all hours with no human activity on the coal pile.

Concentration	Site 2		Site 3	
	PM _{2.5} Mean/Max.	PM ₁₀ Mean/Max.	PM _{2.5} Mean/Max.	PM ₁₀ Mean/Max.
C_{xs} (measured)	2.4/16	14.3/134	3.1/99	11.5/146
C_{xs} (adjusted)	3.5/32	19.7/235	5.9/99	21.1/442

conform to the ambient wind and suggests localized airflow controlled by solar heating of the pile slope. When mixed with ambient cross flow near the top of the pile, these localized airflows can produce vortices that form extreme turbulence and occasionally dust devils.

5.1 Time of Day Variability

The non-linear behavior of $PM_{10} C_{xs}^*$ is illustrated by mean values compared by hour of day. Generally, many meteorological parameters (e.g., wind speed, temperature and relative humidity) vary by time of day so C_{xs}^* . Figure 2a plots the hourly variation in mean C_{xs}^* at both monitoring sites during hours without human activity on the pile and when the wind speed at 10 m was below the wind speed erosion threshold. There are three facts to note. First, there is a tendency for PM_{10} concentrations at site 2 to be greater than values at site 3 (site 2 was nearer the coal pile). Second, there are no data for the hour ending at 1200 LST. Third, the concentration values are typically lowest before 0800 LST. They are highest during 0800-1100 LST, for the hour ending at 1300 LST, and after a slight dip plateau again through 2300 LST. We believe that this pattern reflects the complex interplay of the underlying meteorology: i.e., (1) solar heating rate reaching its maximum at local noon, (2) coal surface temperature reaching a maximum and coal surface moisture content a minimum 2-3 hours later, (3) surface winds at a minimum overnight and increasing to a maximum during the afternoon due to vertical mixing. In addition, the highest levels of excess PM_{10} are consistent with the phenomenon of microscale convective vortices lofting dust clouds during daylight hours. Values of $PM_{10} C_{xs}^*$ when the wind exceeded the erosion threshold are plotted in Figure 2b and indicate that the erosion wind potential was at a maximum during 1800-2300 LST. Data from both sites were combined in Figure 2b because of the low number of observations. Typically, convection and thunderstorm activity reaches a maximum in late afternoon and early evening leading to a greater frequency of gusty outflows reaching the surface and this could explain the evening peak in Figure 2b.

The inhomogeneous nature of the data across all hours can be somewhat ameliorated by smoothing the hourly observations. Figure 3 contains a plot of hourly $PM_{10} C_{xs}^*$ from both sites combined smoothed using a 3-hr running average of the median hourly C_{xs}^* value. This allowed us to replace hours with relatively few observations with results based on more evenly distributed data. Polynomial fits (dashed lines in Figure 3) further emphasize the primary features in the diurnal patterns and provide for a smoother transition between hours. Both functions peak during midday (site 2: $48 \mu g m^{-3}$; site 3: $35 \mu g m^{-3}$) and are lowest at night. At site 2 the decline from midday through evening was more gradual than the rise from morning. Both sites also had a secondary peak of near $30 \mu g m^{-3}$ for the hour ending at 2200 LST.

Not all hours experienced wind erosion. When wind erosion was expected, the combined (sites 2 and 3) $PM_{10} C_{xs}^*$ averaged $8.5 \mu g m^{-3}$ during 0000-0500 LST, $35.2 \mu g m^{-3}$ during 1000-1600 LST and $102.7 \mu g m^{-3}$ during 1600-2300 LST. From this we know that wind erosion had the greatest potential to liberate PM_{10} from the coal pile during the afternoon and evening. Concentration differences between hours with and without wind erosion were not significant except for 1600-2300 LST when non-erosion events averaged $28.4 \mu g m^{-3}$, only 28 percent of that for the wind erosion hours.

Diurnal patterns hint at other factors that may influence natural fugitive emissions. However, time of day only accounts for 13 percent of the variance in C_{xs}^* . Additional environmental information is needed to estimate natural C_{xs}^* levels and to distinguish natural and man-made fugitive dust.

5.2 Particle Concentration Dependencies

This analysis computed hourly meteorological parameters (all but the last 4 listed in Table 3) using only those 1-min values that coincided with 10-m (i.e., level 2) wind directions aligned with the upwind location of the coal pile relative to the downwind monitoring sites. Thus, the mean hourly value $u_{2,n}$ (wind speed at level 2) was computed for those minutes when the wind direction aligned with airflow over the pile toward site n .

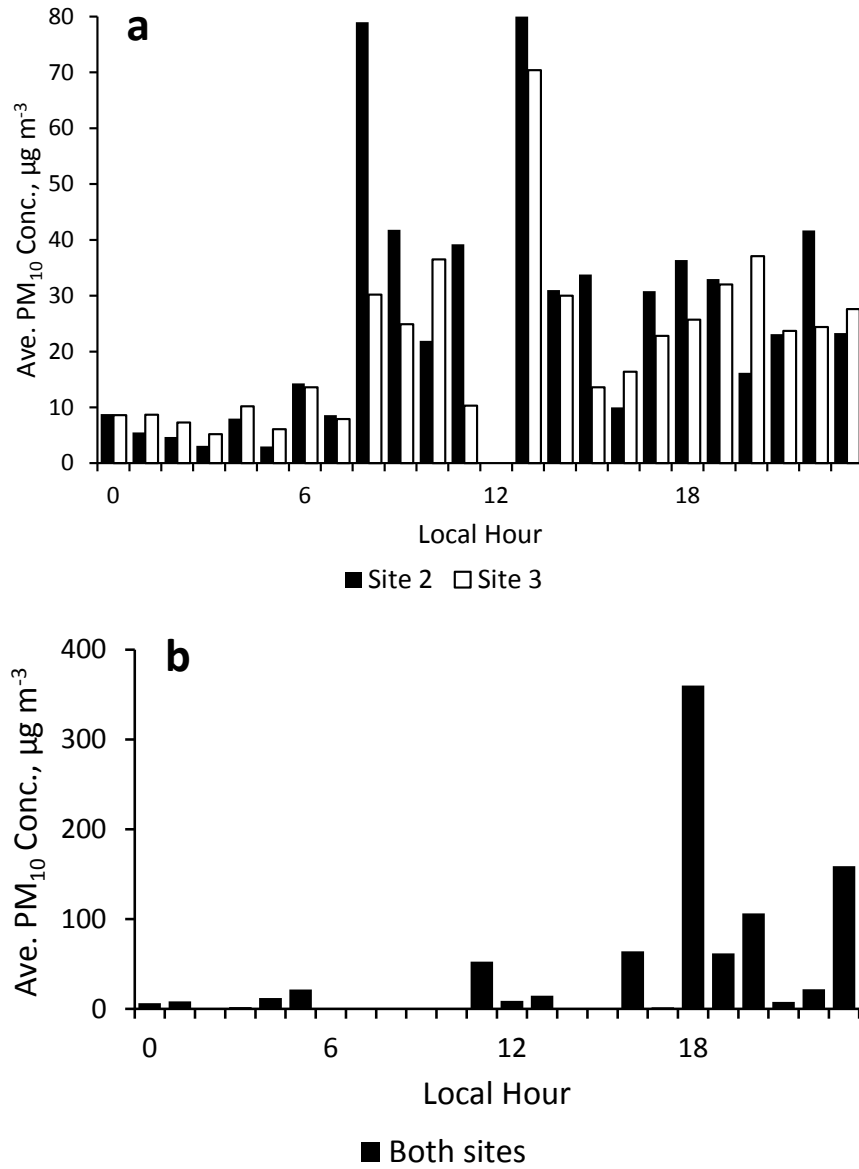


Figure 2. Average PM₁₀ C_{xs}^* by hour of day for hours without human activity on the coal pile and when the 10-m wind speed was (a) below and (b) above the wind erosion threshold. Data from sites 2 and 3 are combined in the bottom plot because of the low number of observations.

The relationship of PM₁₀ C_{xs}^* with pile-aligned meteorological parameters was investigated using multivariate linear regression analysis with stepwise selection of the predictors. Downwind particle concentrations correlate positively with the rate of emission from the pile and negatively with parameters positively associated with diffusion (and secondarily deposition) of transported material.

The general expression for concentration as a function of predictor ρ_i is

$$C_{xs}^* = a_0 + \sum_i a_i \rho_i \quad (5)$$

where a_0 is a constant representing the value of C_{xs}^* when all predictors are zero and a_i is the set of regression coefficients for all predictors. The

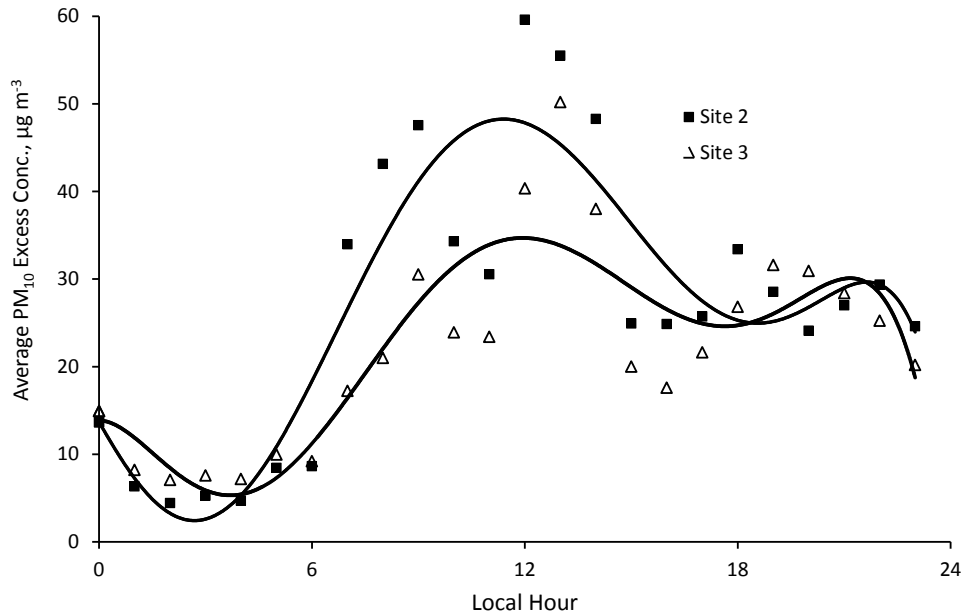


Figure 3. Site-specific time-of-day average values of $PM_{10} C_{xs}^*$ when winds were below the erosion threshold. Averages represent 3-hr running means to smooth the data and reduce variability caused by differences in sample sizes from one hour to the next. Lines (solid=site 2; dashed=site 3) are polynomial fits to the data.

stepwise selection retained only predictors having significance at the 0.10 (p) level or better.

Coal moisture content, M_c , was derived from soil moisture content M_s measured in the ground near the coal pile. The soil measurement 5 cm below the surface represented bulk water in the topsoil layer. Hourly values of M_s varied only slightly throughout the day unless substantial precipitation occurred. Coal samples from the pile were analyzed in a laboratory to determine M_c . A plot of M_s (1000-1600 LST average for each sampling day) versus M_c (Figure 4) shows that daily averages of the two parameters are well correlated ($r^2=0.85$) with M_s experiencing much larger variations than M_c . This relationship provides a means of estimating M_c using M_s as a surrogate.

Table 5a lists the results of this analysis that included 488 data points for hours when the 10-m wind speed was below the erosion threshold defined in AP-42. As expected, average wind speed was not found to be a significant predictor. The 8 parameters identified as being significant represented 25 percent of the total variance in $PM_{10} C_{xs}^*$.

The top four predictors, based on their partial r^2 contributions to C_{xs}^* , are surface (level 1) relative humidity (f_1), fetch across the pile (x_f),

surface air temperature (T_1) and the standard deviation of wind speed at level 2 ($\sigma_{u,2}$). All of these were highly significant and together represented 20 percent of the overall C_{xs}^* variance. The negative association of C_{xs}^* with f_1 was not due to the moisture content of the coal surface because M_s was not identified as a significant predictor. Therefore, f_1 is likely a surrogate for day/night differences in emissions due to the large diurnal variation in f_1 . A similar argument can be made for C_{xs}^* versus T_1 . Note that T_1 is not a surrogate for coal surface temperature T_s because T_1 was not measured directly above the coal pile and T_s responds in a more consistent manner to solar radiation flux than air temperature above the surface (Prigent et al., 2003). In addition, measured solar irradiance failed the regression significance test for a predictor.

The importance of x_f is not as a surrogate for the source surface area because x_f is negatively associated with concentration. As previously discussed, we believe that natural emissions on the pile occur at specific locations on the pile and not across the entirety of exposed coal surface. Instead, it is likely that a negative association between C_{xs}^* and both x_f and x (distance from the pile edge to the

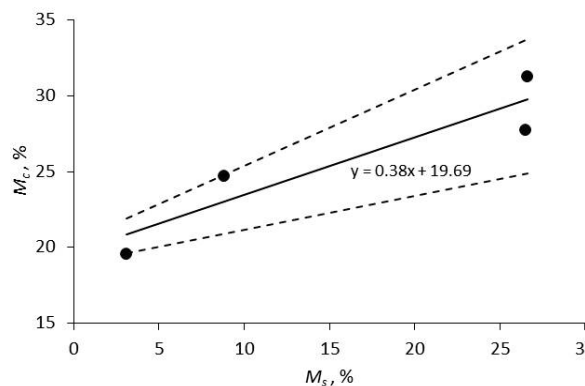


Figure 4. Comparison of sampled values of coal moisture content M_c with nearby measurements of soil moisture content M_s . Solid circles represent daytime M_c sample averages versus M_s data averaged daily for 1000-1600 LST. Dashed lines represent linear fits between maximum (upper) and minimum (lower) daily M_c values versus averaged M_s to illustrate coal moisture variability across multiple daily samples. The solid line is the linear regression of the averages accompanied by the regression equation ($r^2=0.85$).

measurement location) is due to the inverse effects of particle dispersion on distance from the point of emission.

Wind speed varies near the ground as boundary layer eddies intermittently transport momentum downward to the surface. Most turbulence metrics failed as predictors and this is construed to indicate that the tower measurements did not represent turbulence on the pile at the point where dust was generated. We postulate that the value of $\sigma_{u,2}$ as a predictor with positive association is in its representation of the periodicity of boundary layer eddies that acted on the pile surface to enhance dust emissions through specific mechanisms described below.

Concentration increased at the monitoring sites as the value of ΔT (near-ground vertical temperature difference) became more negative. This does not argue in favor of a dispersion effect because the association is in the wrong direction. We believe ΔT is a likely surrogate for general surface heating, similar to but distinctly different from T_1 . Dust emissions show a preference for daytime conditions and ΔT is consistent with that behavior. The last two predictors (σ_{bscat} and ϵ_{TK}^+) are relatively minor

and are not discussed in depth here. The low importance assigned to the 1-min maximum turbulent kinetic energy (ϵ_{TK}^+)—the only turbulence metric to show some significance as a predictor—highlights the difficulty we had using turbulence data to study dust emission rates. One reason for this is the high spatial variability in turbulence that likely occurs over the pile. Another reason is probably the fact that, while turbulence may be a factor positively influencing pile emissions, it also drives particle diffusion in a way that negatively impacts downwind concentrations. These emission and the diffusion effects oppose each other, as was noted by Cowherd et al. (1974), and the net effect is not easily discerned. Overall, the set of predictors did a mediocre job reflecting the full range in downwind concentrations of fugitive PM_{10} when winds were light.

A similar analysis was made of $PM_{10} C_{xs}^*$ for hours with wind erosion. As outlined in AP-42 guidance for coal piles, wind erosion is considered probable when maximum short-term (1-2 min average) wind speeds exceed 5 m s^{-1} . This threshold is based on the lowest published u_t^* value (0.55 m s^{-1}) for crushed coal piles. Hour-average wind speed during the 64 hours (day and night) when $u_{2,r} \geq u_t$ varied between 2.0 and 6.3 m s^{-1} . The predictors of $PM_{10} C_{xs}^*$ under these conditions (Table 5b) were μ^2 , M_s , σ_{bscat} and x_f . Two of the predictors in the presence of wind erosion were also predictors without erosion. Wind speed as represented by μ^2 was clearly a major factor controlling fugitive dust emissions when the erosion threshold was exceeded. Soil moisture content was also a strong predictor for the hours with more wind. This may be due to the fact that, as described by Laurent et al. (2009), moisture content in the coal surface creates stronger cohesive forces on small coal dust particles that are better able to resist erosion by wind action. The overall skill of the statistical model ($r^2=0.65$) when wind erosion was indicated was far greater than that for the lower speed hours.

5.3 Estimating Natural Levels of $PM_{10} C_{xs}^*$

Meteorological parameters provide some value in estimating natural levels of $PM_{10} C_{xs}^*$ downwind of a coal pile. The limited skill of statistical predictors during low wind conditions is presumably due to the highly variable and somewhat stochastic nature of processes (e.g., dust devil and turbulent dust clouds) that produce airborne particulate matter over the coal

Table 5. Results from a multivariate linear regression of $PM_{10} C_{xs}^*$ for hours without human activity on the coal pile.

(a) 10-m wind speed < erosion threshold (488 hours, data from sites 2 and 3 combined)

Predictor ^a (ρ)	ρ Level	Partial r^2	a	Interpretation of Effect (E = emission & D = dispersion)
f_1	<0.0001	0.092	$-0.63 \mu\text{g m}^{-3} \%^{-1}$	Daytime E > nighttime E
x_f	<0.0001	0.044	$-0.083 \mu\text{g m}^{-3} \text{m}^{-1}$	D increases with distance
T_1	<0.0001	0.034	$0.91 \mu\text{g m}^{-3} \text{K}^{-1}$	Daytime E > nighttime E
σ_u	<0.0001	0.029	$69.7 \mu\text{g m}^{-3} (\text{m s}^{-1})^{-1}$	E increases with wind gustiness
ΔT	0.0007	0.021	$-11.2 \mu\text{g m}^{-3} \text{K}^{-1}$	E increases with surface heating
x	0.0014	0.019	$-0.068 \mu\text{g m}^{-3} \text{m}^{-1}$	D increases with distance
σ_{bscat}	0.049	<0.01	$0.64 \mu\text{g m}^{-3} \text{Mm}$	E increases with frequency of disturbances
ϵ_{TK}^+	0.098	<0.01	$-40.4 \mu\text{g m}^{-3} (\text{m}^2 \text{s}^{-2})^{-1}$	D increases with turbulence

(b) 10-m wind speed \geq erosion threshold (64 hours, data from sites 2 and 3 combined)

Predictor ^a (ρ)	ρ Level	Partial r^2	a	Interpretation of Effect (E = emission & D = dispersion)
μ^2	<0.0001	0.470	$5480 \mu\text{g m}^{-3} (\text{m s}^{-1})^{-2}$	E increases with P_w
M_s	0.0003	0.110	$-2.27 \mu\text{g m}^{-3} \%^{-1}$	E increases as coal surface dries
x_f	0.028	0.036	$-0.142 \mu\text{g m}^{-3} \text{m}^{-1}$	D increases with distance
σ_{bscat}	0.031	0.032	$4.75 \mu\text{g m}^{-3} \text{Mm}$	E increases with frequency of disturbances

^aSee Table 3 for an explanation of predictors. All predictors other than M_s are based on minutes when the source and downwind monitoring sites were aligned. All wind-related predictors are based on measurements only at the upper level.

^bCoal moisture content was strongly associated with M_s based on data collected from the coal pile.

pile. In addition, some events on or near the coal pile may have occurred that were not captured on camera and data from these events may have made it more difficult to quantify the relationship between boundary layer meteorology and downwind dust levels.

Review of C_{xs}^* predictors for data from specific monitoring locations revealed that different predictors were selected to represent each site. Regression r^2 values computed by site were similar to or greater than those for the models of the joint data set. Results summarized in Table 6 indicate that there were no common predictors across all models. For hours when wind speed $u_{2,n}$ was below the erosion threshold u_b , C_{xs}^* models for sites 2 and 3 shared only the f_1 and T_1 predictors. However, the u and σ_u^+ predictors for low $u_{2,n}$ hours at site 2 represent atmospheric characteristics that are similar to what is represented by the σ_u^+ , σ_w and

σ_w^+ predictors for site 3. Both sets of parameters characterize boundary layer transport and turbulence, so clearly such turbulence plays an important role in influencing C_{xs}^* although the signs of the coefficients are not all in agreement.

Somewhat better statistical modeling results were obtained when data from both sites were combined and hours were limited to midday periods when the turbulent emissions were expected to be most prevalent and the wind erosion criterion was not met. For the subset of hours between 0900 and 1800 LST, the predictors identified were σ_{bscat} , T_1 , x , u_2 and σ_{u2}^+ . This is the only model ($r^2=0.39$) for low wind speed hours in which wind speed was a significant positive predictor of C_{xs}^* , probably because it eliminated nighttime hours when speed is relatively low and uniform. We believe that σ_{bscat} represents the intensity of turbulent

Table 6. Predictors of $PM_{10} C_{xs}^*$ for hours with no human activity on the coal pile and with data sorted by monitoring site and potential for wind erosion.^a

Predictor ^b	Site 2				Site 3			
	No wind erosion		Wind erosion		No wind erosion		Wind erosion	
	Partial r^2	a^c	Partial r^2	a^c	Partial r^2	a^c	Partial r^2	a^c
f_1	0.121	-0.785			0.090	-0.475		
T_1	0.022	0.998			0.030	0.888		
ΔT	0.057	-17.1						
u	0.017	11.1						
σ_u^+	0.011	-33.3			0.041	-33.2		
μ^2			0.155	2267			0.574	8009
σ_w					0.011	209		
σ_w^+					0.026	-83.4		
σ_{bscat}			0.585	8.58	0.017	0.818		
x_f	0.095	-0.114	0.075	-0.165				
M_s							0.098	-306
Total $r^2=$	0.32		0.81		0.22		0.67	

^aValues shown in bold are for predictors with confidence levels ≥ 99 percent. Other predictors have confidence levels ≥ 90 percent but < 99 percent.

^bPredictors are defined in Table 3.

^cRegression coefficient expressed in $\mu g m^{-3}$ per unit change in predictor.

disturbances moving across the coal pile, similar to its representation of man-made disturbances during a previous study (Mueller et al., 2013). However, the negative association of C_{xs}^* with σ_{u2}^+ is not understood and seems to contradict the positive association with σ_{bscat} .

Models for hours with wind erosion (i.e., when $u_{2,r} \geq u_t$) shared μ^2 —the surrogate for the squared term in the expression for P_w in (1)—as a common predictor. Clearly, wind erosion represented by P_w is a principal factor controlling downwind dust concentrations during the hours with stronger winds. At site 2 the other predictors were σ_{bscat} and x_f . The former captures the intensity of the wind disturbance over the coal pile while the latter represents the decay in concentration with transport distance. The only predictor besides μ^2 at site 3 was M_s . It is not obvious why surface moisture was not significantly associated with C_{xs}^* at both sites.

Overall, mean $PM_{10} C_{xs}^*$ was highest for hours with wind erosion and, in the absence of wind erosion, higher during the daytime hours (Table 7). The highest PM_{10} values (average of $41.5 \mu g m^{-3}$) for wind erosion conditions occurred late in the day (1800-2300 LST). These hours were sometimes associated with outflow winds from nearby afternoon/evening thunderstorms. At least one such event was captured by the surveillance camera. Midday PM_{10} levels for hours with low winds but a high probability of dust erosion by turbulent eddies averaged nearly twice that of other hours with low winds. Note that, unlike PM_{10} , average $PM_{2.5} C_{xs}^*$ was not highest for hours when wind erosion was important but was instead greatest during the daytime for low wind speed conditions. It appears that wind erosion has little impact on $PM_{2.5}$ emissions, consistent with Harris and Davidson (2009).

Table 7. Average C_{xs} by conditions at the coal pile (site 2 and 3 data combined)

Condition	Average C_{xs} , $\mu\text{g m}^{-3}$	
	PM _{2.5}	PM ₁₀
Pre-0900 LST or post-1800 LST—no wind erosion	4.5	16.4
0900-1800 LST—no wind erosion	8.7	28.8
All hours with wind erosion	4.9	41.5

5.4 Downwind Levels of PM_{2.5} C_{xs} *

Fine (PM_{2.5}) particle levels downwind of the coal pile were more difficult to study due to the lower levels that occurred. Downwind-upwind differences at both sites for low and high wind speed conditions are plotted in Figure 5a, sorted into the same time-of-day categories used to examine PM₁₀ C_{xs} * (Figure 5b) in the previous section. “Invalid” denotes PM_{2.5} differences that indicated upwind concentrations were significantly greater than downwind values, while “~0” denotes values that are $0 \pm 4 \mu\text{g m}^{-3}$. Most PM_{2.5} C_{xs} * values were near zero and the differences between frequency distributions for the two time-of-day data sets were small. Large day-night differences between PM₁₀ C_{xs} * values (Figure 5b) are not primarily attributable to PM_{2.5} differences because daytime PM_{2.5} C_{xs} * averages $4.3 \mu\text{g m}^{-3}$ higher whereas daytime PM₁₀ C_{xs} * averages $12.4 \mu\text{g m}^{-3}$ higher. This implies that unmeasured smoke plumes from coal fires—which contribute to the PM_{2.5} mass fraction—were not the primary reason for the time-of-day differences in low-wind PM₁₀ levels.

Given the large PM₁₀ versus PM_{2.5} C_{xs} * differences, it is safe to assume that smoke did not contribute substantially to the considerable low-wind PM₁₀ C_{xs} * levels measured before 0900 and after 1800 LST. To verify this conclusion we eliminated all hours when PM_{2.5} and PM₁₀ C_{xs} * were both $\leq 4 \mu\text{g m}^{-3}$ to focus only on periods when a valid downwind particulate excess was identified (i.e., excess concentrations were both above the minimum threshold for determining non-zero levels). We identified no significant association between PM_{2.5} and PM₁₀ in measurements from either site. The median PM_{2.5}/PM₁₀ ratios were 0.25 (site 2) and 0.37 (site 3). These ratios are far greater than the 0.10 reported by EPA (1995) for unpaved surfaces and the ratios found

downwind of a dry fly ash storage facility (i.e., <0.10) where it was determined that ash disposal produced non-zero fugitive dust emissions in both the PM_{2.5} and PM_c (=PM₁₀-PM_{2.5}) size ranges (Mueller et al., 2013).

With no statistical association between fine and coarse particle mass and given PM_{2.5}/PM₁₀ ratios that appear too large to represent purely fugitive sources, it appears that the presence of excess PM_{2.5} mass at the downwind monitoring sites was generally not attributable to mechanically-generated fugitive dust emissions from the pile. An alternate hypothesis for the few remaining unexpectedly high PM_{2.5} values (i.e., $>5 \mu\text{g m}^{-3}$) measured during a few hours was smoke from coal dust combustion on the pile. Unfortunately, no coal fire data base exists so this hypothesis is based on informal observations of small smoldering fires during infrequent site visits. However, one major fire was observed on camera and the PM_{2.5} concentrations (not “excess” but total) during that period were as high as $79 \mu\text{g m}^{-3}$ and the PM_{2.5} fraction of PM₁₀ was as high as 0.96. We showed earlier that there were fewer hours compared to PM₁₀ when downwind PM_{2.5} levels were significantly greater than those upwind. This indicates that the signal of a PM_{2.5} fugitive emission from the coal pile was usually very small. These factors made it impossible to further separate and quantify PM_{2.5} fugitive dust emissions from natural mechanical processes and human activity. It is possible that in extreme cases coal pile smoke could have affected PM₁₀ concentrations thereby adding to uncertainty in identifying relationships between observed PM₁₀ concentrations and local meteorological parameters.

6. CONCLUSIONS

Atmospheric processes frequently enhanced PM₁₀ levels in air passing over a coal pile. Direct entrainment of particulate matter into the air by ambient wind was clearly detected for the small fraction of hours when 1-min wind speed values exceeded the estimated erosion threshold. Wind erosion was not a function of the fetch across the pile, implying that it occurred at specific locations such as previously reported for the leading and lateral edges of the elevated portion of a pile. However, for most hours of this study the mean ambient wind was not sufficient to cause erosion of coal dust.

Observations identified dust devils forming and moving across the coal pile. This is

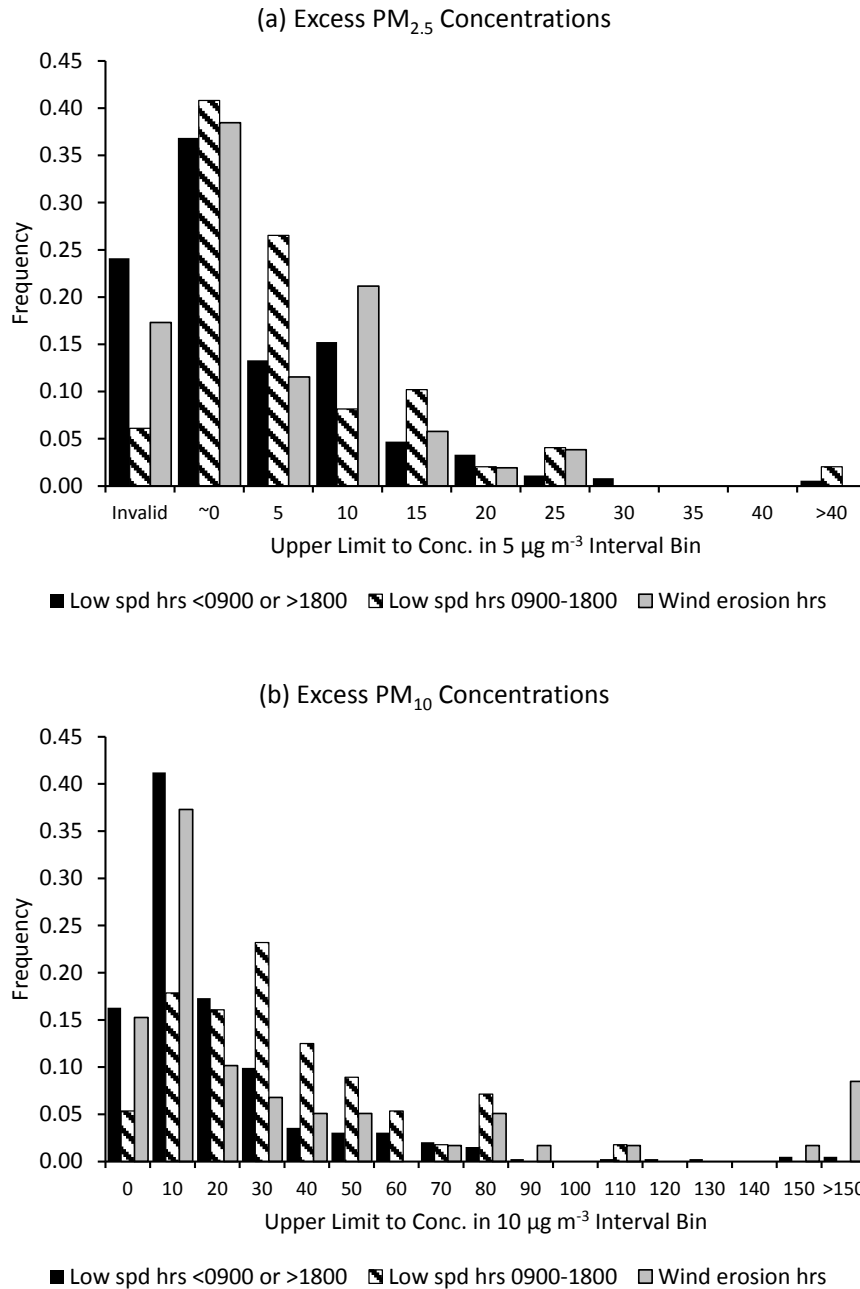


Figure 5. Frequency distributions of $PM_{2.5}$ and PM_{10} C_{xs}^* for low speed (i.e., no wind erosion) hours sorted into two different time periods and for all wind erosion hours combined. In graph (a), “Invalid” refers to hours with $PM_{2.5}$ $C_{xs}^* \leq -4 \mu g m^{-3}$ and “~0” refers to all values that are statistically zero, or $0 \pm 4 \mu g m^{-3}$. Most data in plot (a) are sorted into bins that $5 \mu g m^{-3}$ in size while plot (b) data are sorted into $10 \mu g m^{-3}$ bins.

evidence that the pile produces its own turbulent flows capable of raising dust from its surface even when ambient wind speeds are relatively low. Detailed statistical analysis during low ambient wind speeds of dust levels versus

associated meteorological factors implicates the action of turbulent airflow as the primary source of excess PM_{10} mass at downwind measurement sites. We are unable to express generalities about how excess concentrations

vary using a common set of specific predictors across all events. Time of day and wind erosion potential seem to be the best predictors of concentration at combined sites (Table 7). Excess PM₁₀ levels are lowest at night when boundary layer turbulence is at a minimum, wind speeds are low and there is no direct solar heating of the pile. These levels typically reach a maximum around midday and vary with light scattering and wind behavior measured downwind of the pile. Evidence is weak for the influence of coal surface moisture on dust erodibility in the absence of human activity, perhaps because of limited variation in its surrogate (M_s) during the hours examined.

Excess concentrations of PM_{2.5} were not well correlated with PM₁₀ mass and were usually not sufficiently high to identify non-zero levels with confidence. Excess PM_{2.5} values were lowest at night. The difference between the low speed (i.e., no wind erosion) midday hours (8.7 $\mu\text{g m}^{-3}$) and wind erosion hours (4.9 $\mu\text{g m}^{-3}$) was unexpected and cannot be explained. Of the processes that potentially contribute to an excess of particulate matter downwind of a coal pile, coal fires probably make an occasional contribution to PM_{2.5} levels but are unlikely to have much influence on airborne PM₁₀ mass. Overall, the data do not suggest a significant, measureable PM_{2.5} contribution to downwind particle levels from atmospheric processes and this is consistent with previous studies that indicate most wind erosion occurs for particles in the 5-10 μm size range.

Wind erosion alone is unable to explain all natural particulate emissions from the coal pile because of the significant mean values of PM₁₀ C_{xs}^* across all wind speeds and hours. Localized airflow accelerations due to solar heating of the coal pile itself are the most plausible explanation for daytime hours but fail to explain nighttime values. Nighttime low-wind PM₁₀ values, though much lower, might be caused by unseen activity near the pile, could be due to a poor representation of background PM₁₀ concentrations, or they may be caused by an unidentified phenomenon. In any event, they are not associated with bulldozer action on the coal pile. Therefore, future use of these data to quantify emission factors from bulldozer activity must avoid including the unexplained particulate levels in emission factor calculations.

7. ACKNOWLEDGMENTS

Funding for this work was provided by the Electric Power Research Institute and the Tennessee Valley Authority.

8. REFERENCES

- Cowherd, C. Jr., K. Axetell, Jr., C.M. Guenther, and G.A. Jutze, 1974: Development of Emission Factors for Fugitive Dust Sources. Midwest Research Institute report, EPA-450/3-74-037, 172 pp (available from <http://www.epa.gov/nscep/index.html>).
- EPA, 1978: Coal Refuse Piles, Abandoned Mines and Outcrops, State of the Art. Industrial Environmental Research Laboratory, EPA-600-2-78-004v.
- EPA, 1995 (with subsequent updates): Compilation of Air Pollutant Emission Factors - Volume I: Stationary Point and Area Sources. AP-42 Fifth Edition, Office of Air Quality Planning and Standards, Research Triangle Park, NC. (<http://www.epa.gov/ttn/chief/ap42>)
- Gillette, D., D. Ono, and K. Richmond, 2004: A combined modeling and measurement technique for estimating windblown dust emissions at Owens (dry) Lake, California. *J. Geophys. Res.* **109**, doi:10.1029/2003JF000025.
- Harris, A.R., and C.I. Davidson, 2009: A Monte-Carlo model for soil particle resuspension including saltation and turbulent fluctuations. *Aerosol Sci. Technol.* **43**, 161-173.
- Laurent, B., B. Marticorena, G. Bergametti, I. Tegen, K. Schepanski, and B. Heinold, 2009: Modelling mineral dust emissions. *IOP Conference Series, Earth and Environmental Science* **7**, doi:10.1088/1755-1307/7/1/012006.
- Mueller, S.F., J.W. Mallard, Q. Mao, and S.L. Shaw, 2013: Fugitive particulate emission factors for dry fly ash disposal. *J. Air & Waste Manage. Assoc.* **63**, doi:10.1080/10962247.2013.795201.
- Nugroho, Y.S., R.R. Rustam, Iman, and M. Saleh, 2008: Effect of humidity on self-heating of a sub-bituminous coal under adiabatic conditions. Ninth International Symposium of Fire Safety Science, International Association for Fire Safety Science, doi:10.3801/IAFSS.FSS.9-179.
- Ono, D., 2006: Application of the Gillette model for windblown dust at Owens Lake, CA.

- Atmos. Environ.* **40**, doi:10.1016/j.atmosenv.2005.08.048.
- Perera, I.E., and C.D. Litton, 2011: A detailed study of the properties of smoke particles produced from both flaming and non-flaming combustion of common mine combustibles. *Fire Safety Science* **10**, doi:10.3801/IAFSS.FSS.10-213.
- Prigent, C., F. Aires, and W.B. Rossow, 2003: Land surface skin temperatures from a combined analysis of microwave and infrared satellite observations for an all-weather evaluation of the differences between air and skin temperatures. *J. Geophys. Res.* **108**, doi: 10.1029/2002JD002301.
- Renno, N.O., M.L. Burkett, and M.P. Larkin, 1998: A simple thermodynamic theory for dust devils. *J. Atmos. Sci.* **55**, 3244-3252.
- Saxton, K., D. Chandler, L. Stetler, B. Lamb, C. Claiborn, and B.-H. Lee, 2000: Wind Erosion and fugitive dust fluxes on agricultural lands in the Pacific Northwest, *Transactions of the ASAE* **43**(3), 623-630.
- Turpin, C., and J.-L. Harion, 2009: Numerical modeling of flow structures over various flat-topped stockpiles height: implications on dust emissions. *Atmos. Environ.* **43**, doi:10.1016/j.atmosenv.2009.07.047.
- Watson, J.G., J.C. Chow and T.G. Pace, 2000: *Air Pollution Engineering Manual*, W.T. Davis (ed.), Chapter 4 - Fugitive Dust Emissions, Air & Waste Manage. Assoc., 117-135.